DESIGN OF A PERPENDICULAR BIASED 2ND HARMONIC CAVITY FOR THE FERMILAB BOOSTER *

C.Y. Tan†, J.E. Dey, K.L. Duel, J.C. Kuharik, R.L. Madrak, W.A. Pellico,
E.J. Prebys, J.S. Reid, G. Romanov, D. Sun, I. Terechkine,
Fermilab, Batavia, IL 60510, USA

Abstract

A perpendicular biased 2nd harmonic cavity is being designed and built for the Fermilab Booster. Its purpose is to flatten the bucket at injection and thus change the longitudinal beam distribution to decrease space charge effects. It can also help with transition crossing. A model cavity has been built to verify various CST Microwave studio and COMSOL modeling results. A test stand has been built to verify that the Y567 tube is able to operate at twice the Booster fundamental frequencies. Also discussed are the RF windows which are critical to the design.

INTRODUCTION

The goal of the perpendicular biased 2nd harmonic cavity currently being designed and built at Fermilab is to improve the capture and transition efficiency of Booster [1]. However, perpendicular biased cavities are technically difficult to build for a rapid cycling machine. To this date, no perpendicular biased cavity that has a large frequency sweep (29 MHz for our purposes) and a gap voltage of 100 kV has been made operational. The technical challenges in this project are multifold and some of them will be addressed in this paper.

CAVITY MODEL

The cavity model is constantly updated while work on it is progressing. A very important change in the cavity design was the implementation of RF power source. Still the most effective RF amplifier concept proposed in [2] was used with the same power tetrode 4CW150000E (see Fig.1). The volume of 2nd harmonic cavity is relatively small, so the impact of the connected power tube cavity was significant. A number of adjustments were made to restore the operating frequency and tuning range.

Yet most of the recent modifications done in the cavity design were related to the mitigation of total heating and local hotspots. The tuner now consists of garnet/alumina rings sandwiched together to form a stack. Alumina rings between the garnet ones conduct heat away from the garnet. An extra garnet shim has been added to the face of the garnet stack that improves the bias H-field distribution and thus decreases the temperature of the hotspots. These critical improvements from our prior design [3] are described in more details below.

* Operated by Fermi Research Alliance, LLC under Contract No. DE-AC02-07CH11359 with the United States Department of Energy.
† cytan@fnal.gov

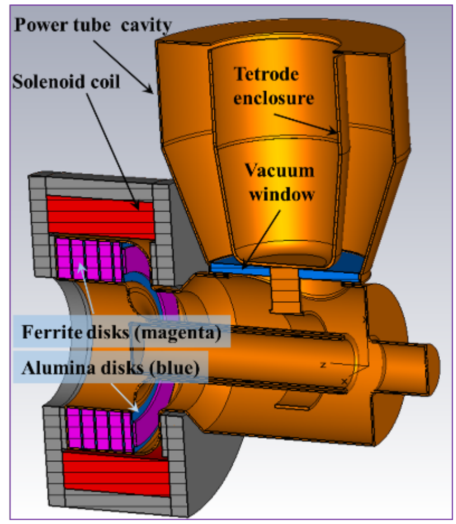

Figure 1: The general view of the current cavity design.

Optimization of Magnetic Field Distribution

The high RF power loss in the tuner is closely associated with the low level of the static magnetic field in the garnet and resulting sharp increase of local magnetic permeability (both the real and the imaginary parts) in the vicinity of the gyromagnetic resonance. One of the ways to improve the quality of the field is magnetic shimming. Shimming the poles of the flux return of the bias magnet does not provide desirable effects because of the big gap between the pole and the garnet material. Another option is using shims installed in the close vicinity of the garnet. In this case, the material of the shims must be low loss, so using the same type of garnet looks like a natural choice. Some modest optimization efforts resulted in the shape of the shim shown in Fig. 2: the ring-shaped shim is 3.5 mm thick with 115 mm inner radius and 148 mm outer radius.

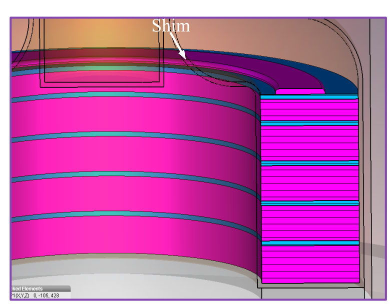

Figure 2: Magnetic shim on the tuner stack.

ISBN 978-3-95450-147-2

Adding the shim resulted in significant improvement in the uniformity of the magnetic field and permeability in the garnet – the peak power loss density at 75 MHz decreased from 55 W/cm^3 to 21 W/cm^3. Also at lowest expected bias current, the minimum value of the magnetic field has increased from ~33 Oe to ~50 Oe. Thus, no direct gyromagnetic resonance condition exists in the garnet material anymore [4]. Further optimization of the shim shape pursued decreasing of the RF electrical field between the shim and the inner electrode of the cavity which caused anomalous heating of the neighboring alumina disk.

Thermal Analysis

Evaluation of the thermal losses in the garnet tuner using a simplified approach based on averaged and integral values for the tuner as a whole may be very misleading. RF loss power density the ferrite strongly depends on the internal magnetic field, which is extremely non-uniform in some areas of the tuner, and so is the RF loss power density. On the other hand, the internal magnetic field is a function of static permeability of the material, which strongly depends on the level and distribution of applied bias magnetic field. And finally the internal field and RF losses distributions depend on time according to the required frequency and amplitude ramp for the 2nd harmonic cavity. This problem was addressed with methods described in Ref. [5, 6]. The garnet and alumina disks with high RF loss from non-uniformity were subdivided into several areas small enough to assume RF loss is uniform in each area and equal to the spatially averaged static RF loss density at a given excitation current. Based on a series of static RF loss simulations (performed with COMSOL in 2D model for speed and enhanced accuracy) the interpolation formulæ were developed to calculate the power loss density in each area at any current. The data obtained this way allows for a simplified calculation of the time and space-averaged RF loss density in each area and in the tuner as a whole. The input for the thermal model is shown in Fig. 3(a), and the result of the thermal analysis is shown in Fig. 3(b).

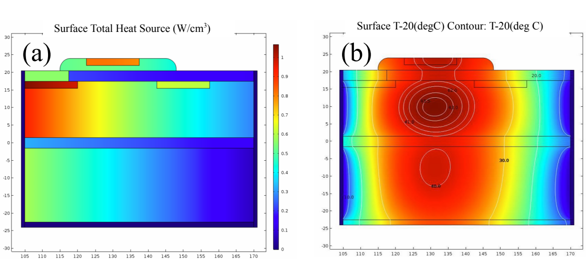

Figure 3: a) A map of the power deposition in the part of the tuner with the shim; b) A temperature map of the same part shows the temperature of the hotspots dropped from 56°C without shim to 44°C with shim.

POWER AMPLIFIER TEST

The Y567B (Eimac/CPI 4CW150000E) tetrode is used in the 38 – 53 MHz power amplifiers (PAs) for the main Booster cavities. Specifications indicate an output power of up to 300 kW with a maximum CW frequency of 108 MHz. Still, it is necessary to verify that the tetrode can run in a stable manner and produce adequate power at the second harmonic frequencies of 76 – 106 MHz. We are currently in the process of testing the PA at maximum possible output power (under sustainable operating conditions), at both 76 and 106 MHz. This required constructing resonators, which, when attached to the PA, resonate at 76 and 106 MHz. In addition, the cathode drive resonator had to be modified in order to perform efficiently at the higher frequencies. This was achieved by simply making the low Q structure shorter.

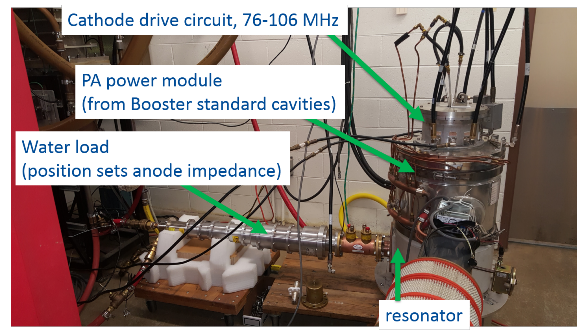

Figure 4: The setup for the 76 MHz PA test.

The first resonator (~ 76 MHz) has already been fabricated. A picture of the test setup is shown in Fig. 4 .The topmost cylinder is the cathode drive circuit. The middle cylinder is the Booster PA power module, which contains the tetrode. The bottom structure is the resonator, formed by a center and outer conductor which are shorted by a plate at the end opposite the power module. The resonator and PA power module are coupled by a ceramic capacitor, and form a quarter wave structure foreshortened by the tetrode output capacitance of 60 pF. A water cooled 50Ω load is attached to the structure at an adjustable tap point. This sets the impedance seen by the anode of the tetrode. The water load also enables measurement of PA output power, given a known water flow and measured temperature change from input to output. A directional coupler in the load transmission line is used to check the calorimetric power measurement.

The existing modulators provide a DC anode voltage of up to 25 kV. Testing proceeded by starting at 18 kV and increasing it to achieve maximum output power. The drive power was adjusted so that the screen current was the same for each modulator DC voltage setting. We have measured 115 kW of output power with 24 kV DC anode voltage (15% duty factor). This was with a suboptimal tap point and anode impedance. After adjusting the anode impedance by moving the load tap point, we measured 112 kW of output power with 18 kV of DC anode voltage at 50% duty cycle. Due to issues with the available drive amplifier, we were limited here. After decreasing the duty cycle to 5 ms/80 ms, the system output power was 160 kW with an anode voltage of 21 kV. This is sufficient given the current plan for operation. Testing is still in progress. Currently, we have ~ 3 kW of drive power available using a spare amplifier, although a dedicated 8 kW drive amplifier is on order. Fabrication of the 106 MHz resonator will begin soon.

AL800 RING

The garnet rings will be manufactured by National Magnetics Group Inc. Due to the size of the ring, it is not possible to make one contiguous ring, so the ring will consist of 8 pieces which are glued together to form a ring. The final garnet ring will have an inner diameter of 210 mm and an outer diameter of 340 mm. These garnet segments will also be glued onto a 3 mm thick alumina (99.5% purity) substrate that has the same inner and outer diameters as the garnet ring. Final machining will be performed on the garnet and alumina assembly after gluing to achieve precise dimensions and flatness, perpendicularity, and parallelism. Figure 5 shows the assembly drawing of the segments and the alumina glued together. Multiple garnet rings will be stacked together to form the cavity tuner.

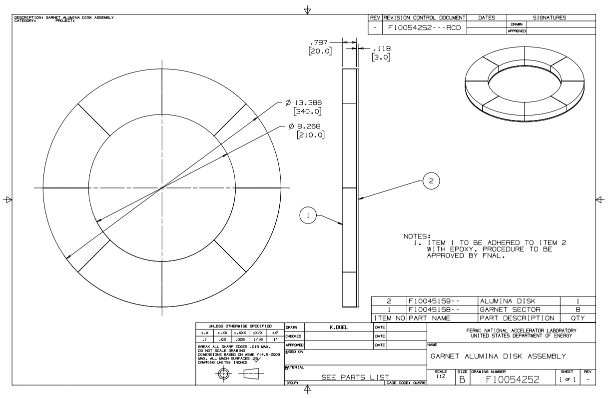

Figure 5: The drawing of the AL800 garnet ring assembly.

RF WINDOWS

RF windows have to be used to separate the vacuum portion of the cavity from the PA and the tuner portion. An RF window is needed in the tuner portion because it will be in a pressurized gas environment,. We use two windows in the design (see Fig. 6) because there is not enough space between the input coupler and the accelerating gap to host a single window. An interesting feature of window A is its location: it will be located inside the cavity. This is due to the limited space in the transition area from the tapered coax line of the coupler to the cavity and other engineering considerations. Simulation results show that window A will have negligible effect on both the coupler and cavity performance. The location of window B has been chosen to avoid possible magnetic field enhanced multipacting/sparking in the tuner area. Both windows will be furnace brazed to form an alumina, copper sleeve sub-assembly that will be welded to the cavity during final assembly.

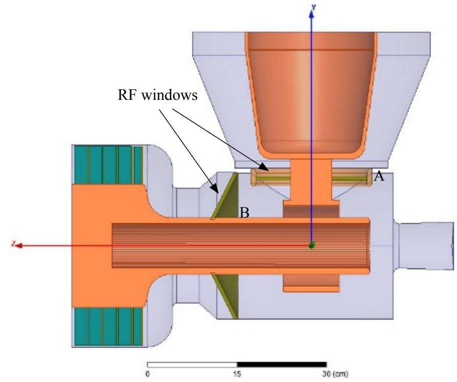

Figure 6: The location of the RF windows A and B are shown here.

CONCLUSION

We have a spent a large amount of work carefully measuring the characteristics of the AL800 garnet. [3] We have used these measurements to improve our design of the tuner. Two garnet rings have been ordered and will be tested to see if they meet our specifications. We have verified that the PA can power the cavity at injection. A new resonator will soon be built to verify that the PA can work at extraction too. We hope to complete our design of the RF windows, solenoid and assembly drawings for the cavity by the end of 2016.

ACKNOWLEDGMENTS

The authors wish to thank F. Caspers, C. Vollinger and S. Clement from CERN for supplying us with information about the gluing process.

REFERENCES

[1] J. M. Kats and W.T. Weng, "Effects of the second harmonic cavity on RF capture and transition crossing", XVth International Conf. on High Energy Accelerators, Hamburg, Germany, July 1992, BNL-45078.

[2] W.R. Smythe et al., "RF Cavities with Transversely biased Ferrite Tuning", in *Proc. 1985 IEEE Particle Accelerator Conference*, p. 2951.

[3] C.Y. Tan et al, "A Perpendicular Biased 2nd Harmonic Cavity for the Fermilab Booster", in *Proc IPAC'15*, WEPTY037.

[4] I.Terechkine and G.Romanov, "Reduction of the RF loss in the Garnet Material of a Tunable Cavity by Optimizing the Magnetic Field Distribution Using Shimming", FNAL TD note TD-16-007, March 2016.

[5] I. Terechkine and G. Romanov, "Thermal Analysis of the Tuner of the FNAL Booster's 2nd Harmonic Cavity", FNAL TD note TD-15-020, Oct. 2015.

[6] I. Terechkine and G. Romanov, "Evaluation of Temperature Distribution in the Tuner of the FNAL Booster's Tunable Second Harmonic Cavity", FNAL TD note TD-16-002, February 2016.

ISBN 978-3-95450-147-2